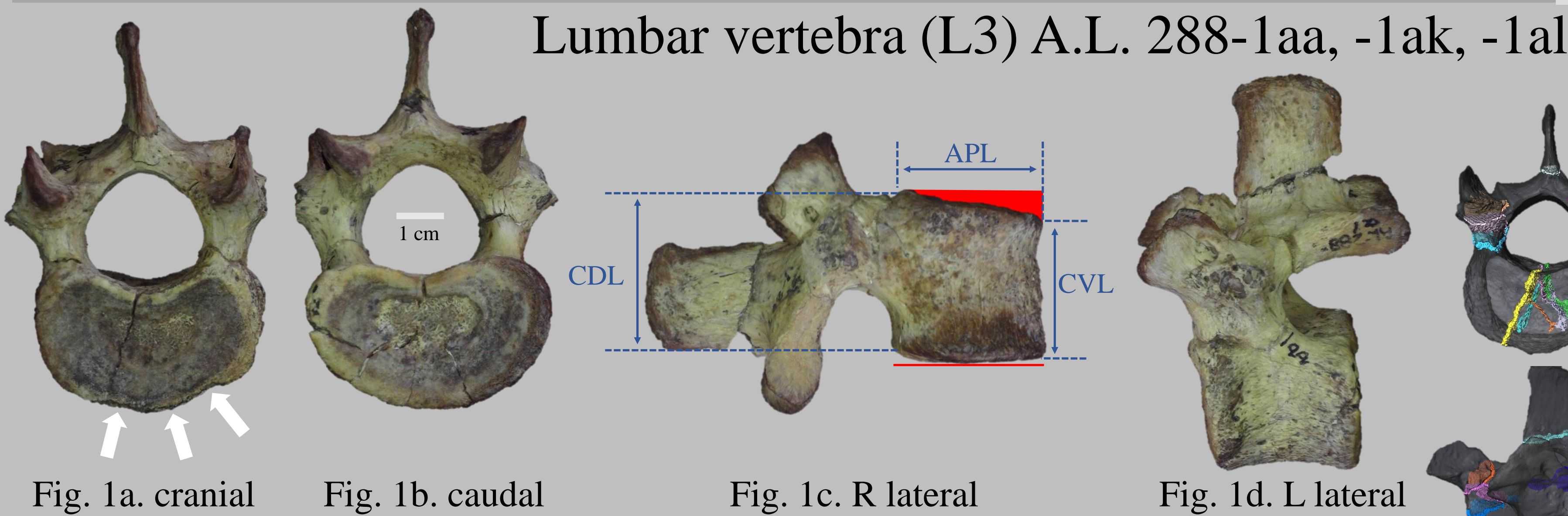
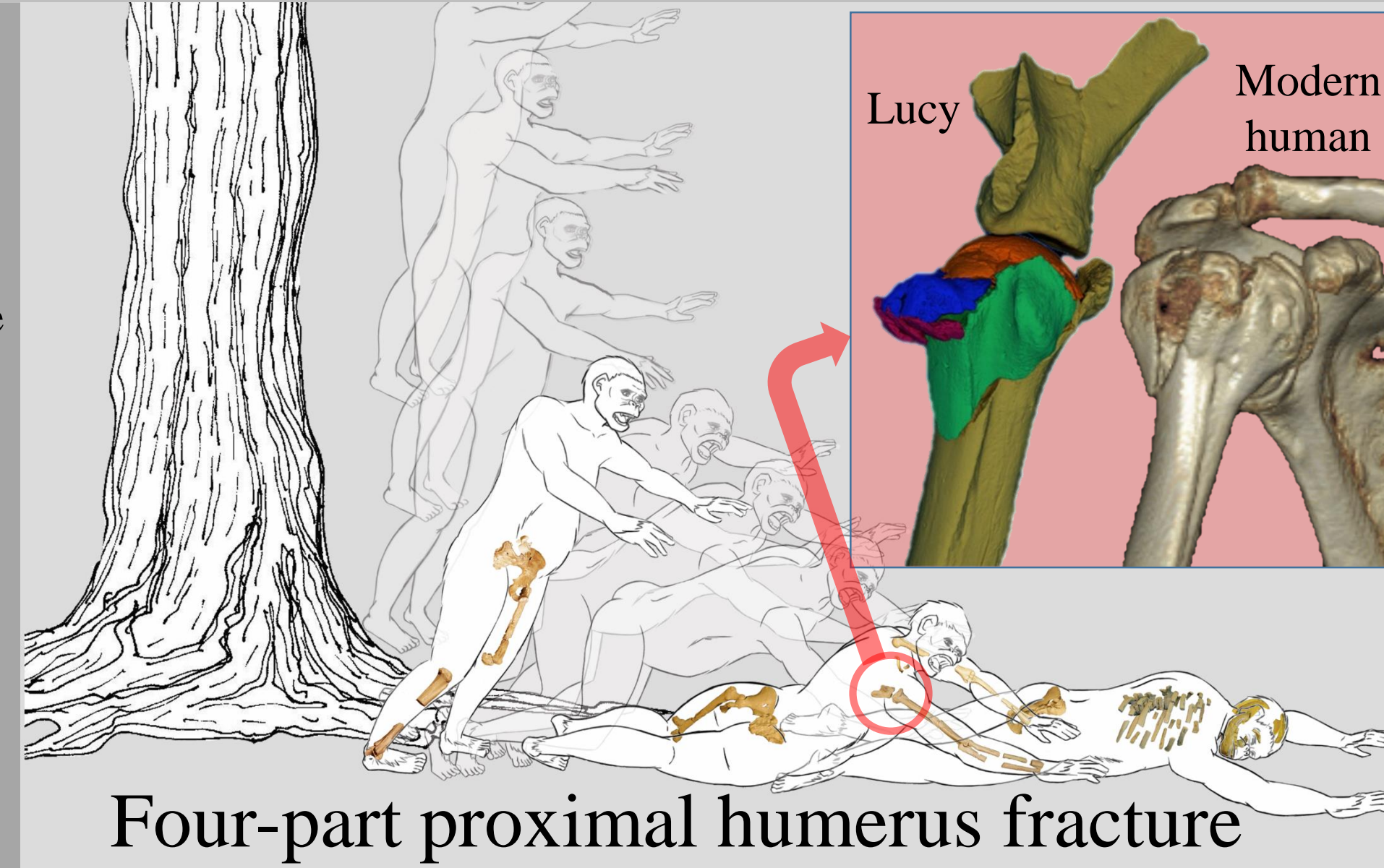


# 3D Fracture Patterns in the Lumbar Vertebra and Tibia of A.L. 288-1 ('Lucy') are Consistent with Perimortem Trauma

S. J. Mattox<sup>1</sup>, C. A. Davis<sup>1</sup>, B. Nachman<sup>1</sup>, D. L. Peterson<sup>2</sup>, W. Akins<sup>3</sup>, M. Feseha<sup>4</sup>, M. Hill<sup>5</sup>, J. Kappelman<sup>1,6</sup>, R. A. Ketcham<sup>6</sup>, L. Todd<sup>1</sup>, and A. Witzel<sup>1</sup>

<sup>1</sup>Dept. Anthropology, UT Austin, TX, <sup>2</sup>Austin Brain and Spine, Austin, TX, <sup>3</sup>Dept. Radio-Television-Film, UT Austin, TX, <sup>4</sup>Paleoanthropology and Paleoenvironment Program, Addis Ababa University, Addis Ababa, Ethiopia, <sup>5</sup>Dept. of Anthropology, Iowa State University, Ames, Iowa, and <sup>6</sup>Dept. Geological Sciences, UT Austin, TX

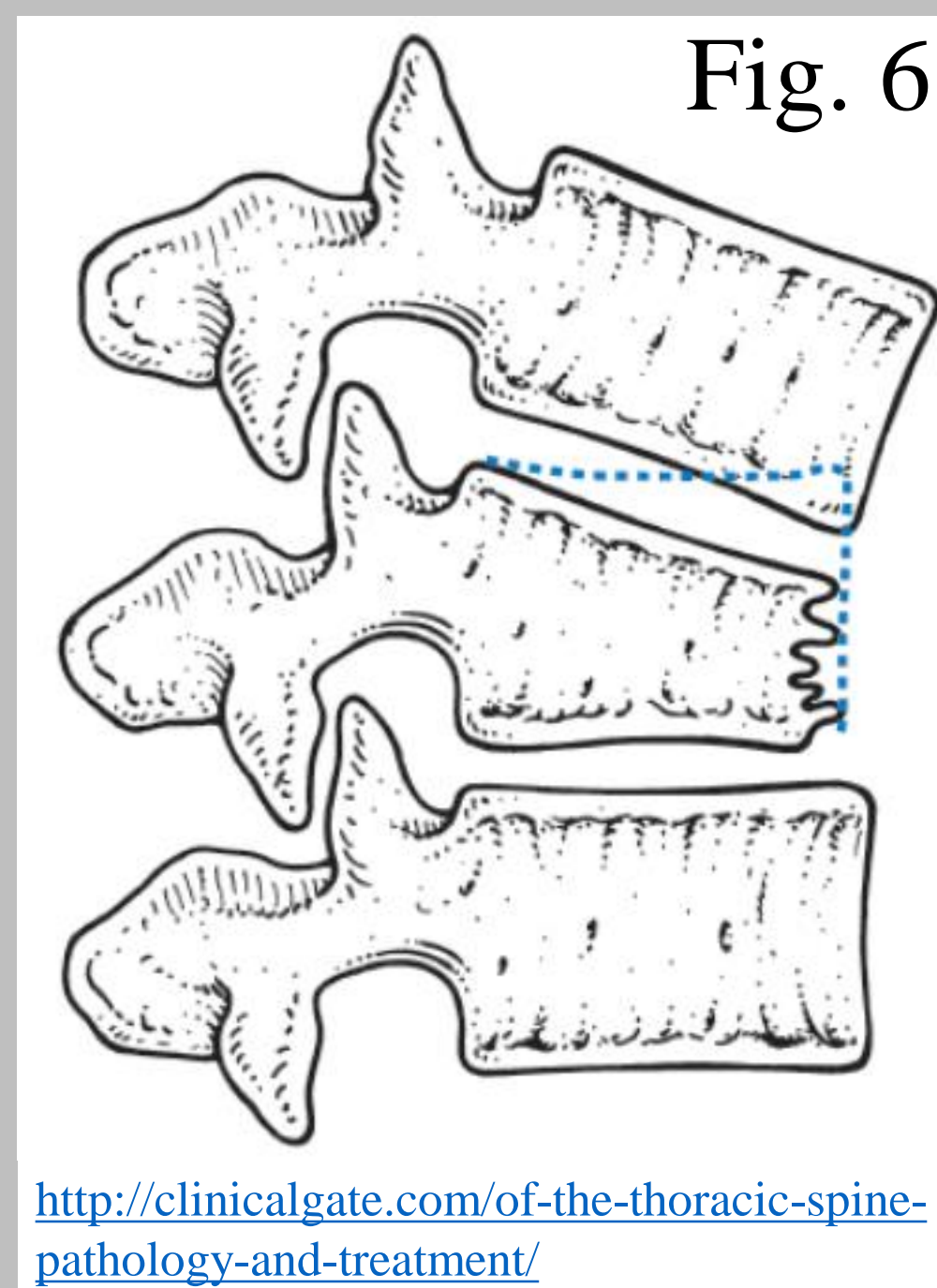
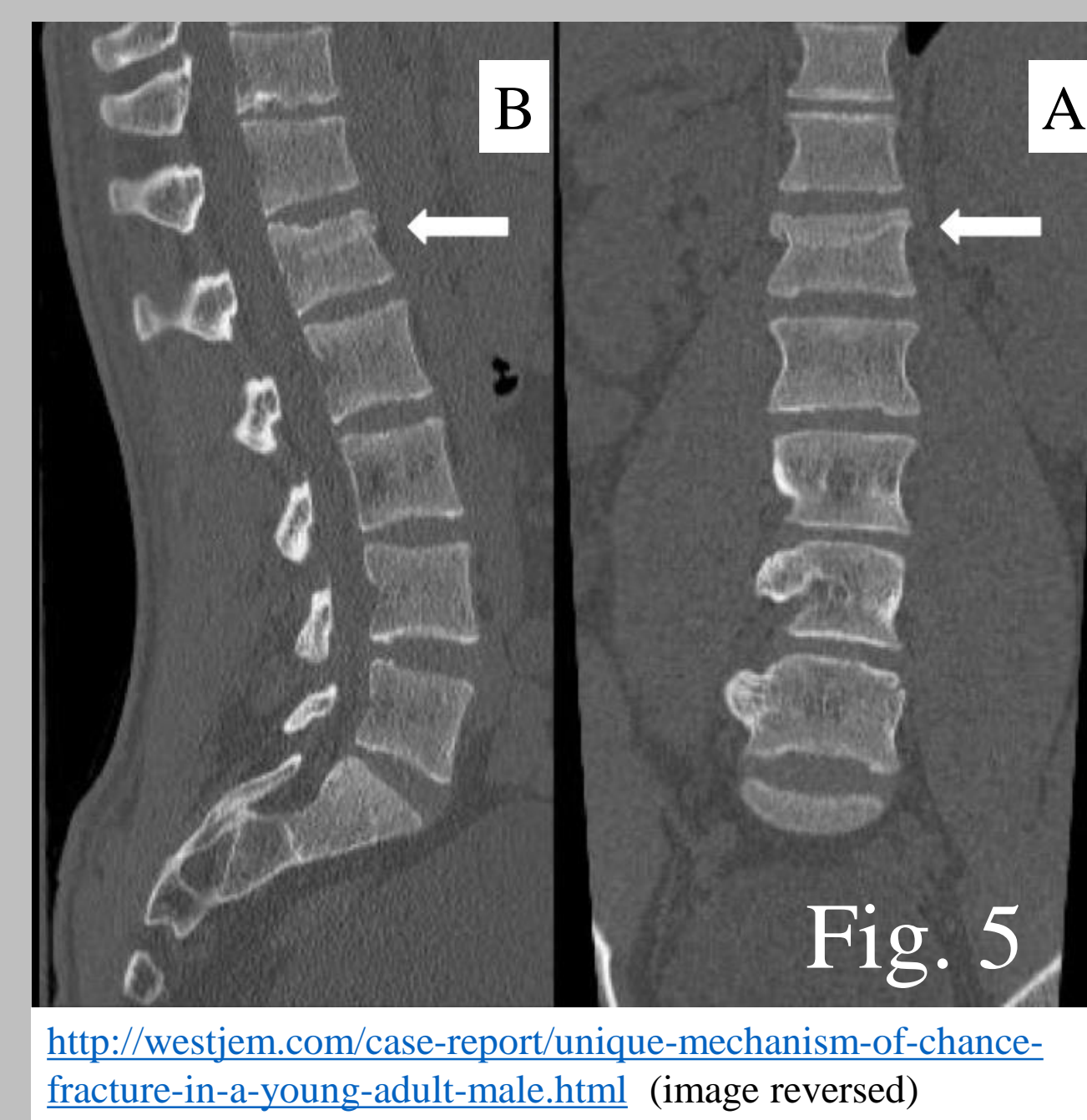
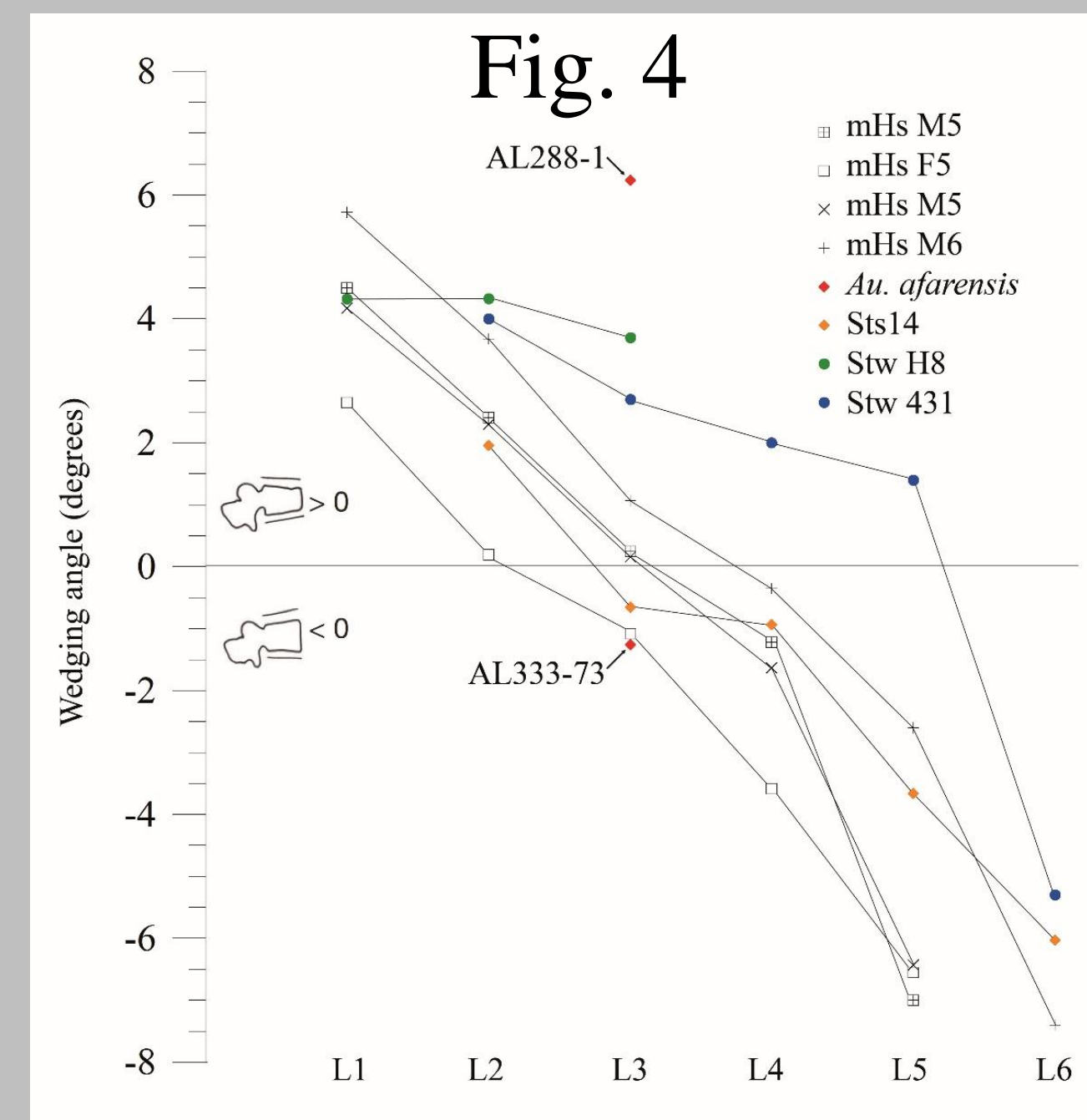
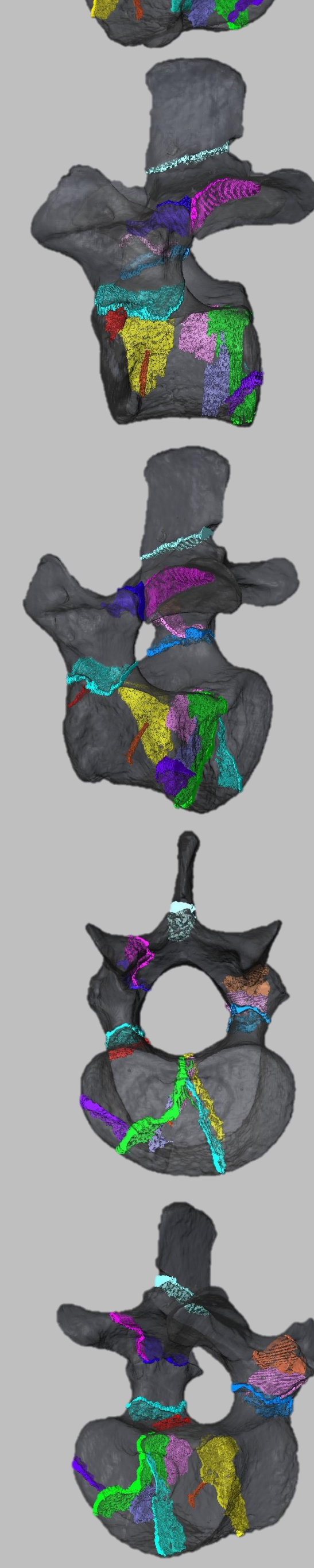
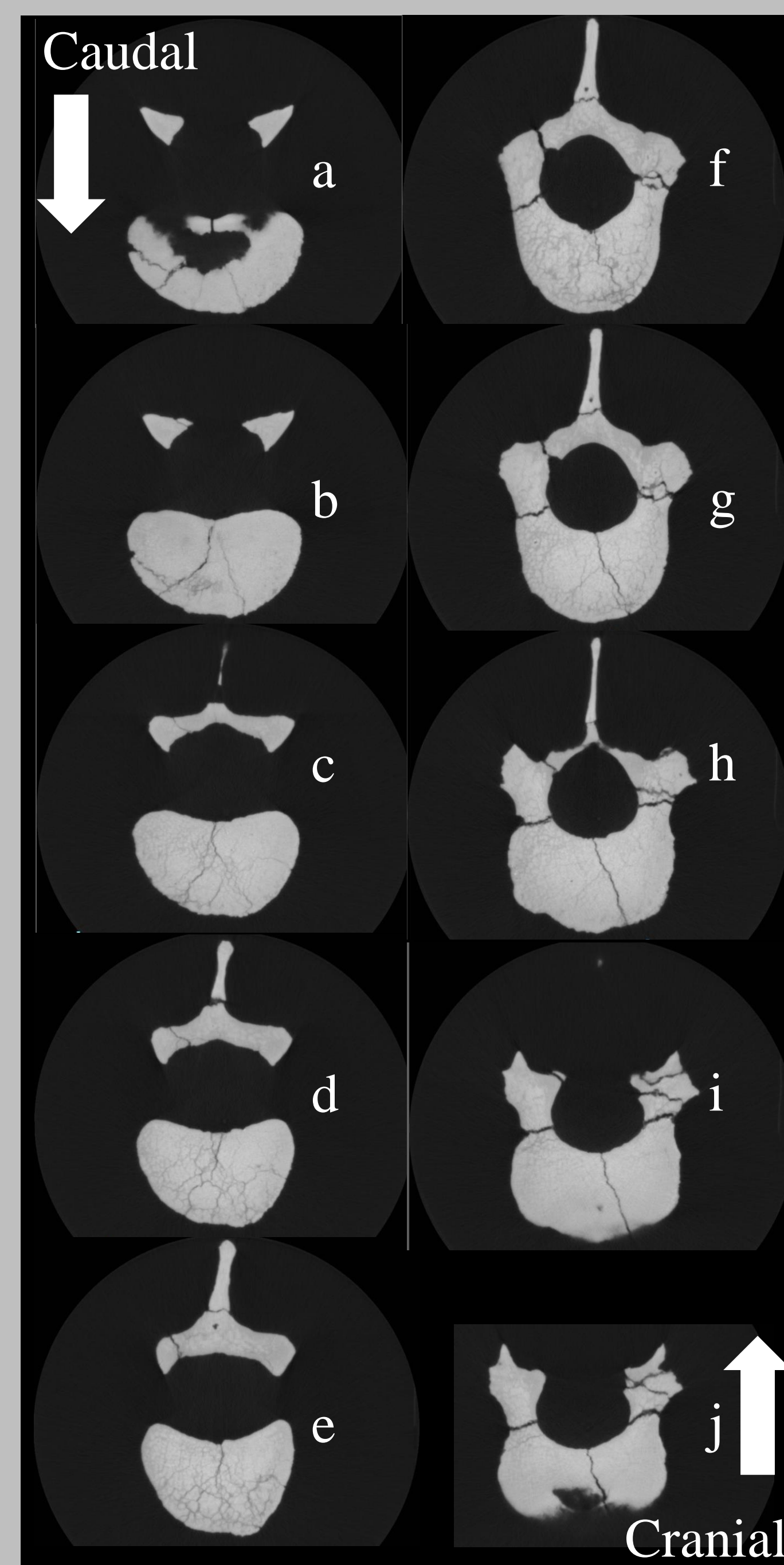
**ABSTRACT.** It was recently hypothesized that A.L. 288-1 ('Lucy') preserves a subset of perimortem fractures consistent with injuries in accident victims who suffer a vertical deceleration event (VDE) (Kappelman et al., 2016). Certain fractures, e.g., a four-part fracture of the right proximal humerus, and a dislocative compressive distal epiphyseal fracture of the left femur, suggest a high velocity impact following a fall from significant height. The severity of these fractures led Kappelman et al. (2016) to hypothesize that other skeletal fractures are also consistent with a VDE. The initial description of A.L. 288-1 (Johanson et al., 1982) detailed many surface "cracks" in other elements that were attributed to fossilization processes. We used high resolution X-ray computed tomography to further investigate the 3D nature of these surface features in two elements, the lumbar vertebra (A.L. 288-1aa,ak,ar), and the right tibia (A.L. 288-1aq,ar). Scans had a slice spacing of 0.05754-0.07044 mm and data volumes were loaded into Avizo (FEI) to produce the 3D element. Fracture planes were mapped in 3D, with planes displayed in color and the element displayed as a transparent object. The lumbar vertebra (likely L3; Meyer et al., 2015) preserves several fractures that appear to communicate through the body between its inferior and superior surfaces that, along with the fractures through the bases of both pedicles, are suggestive of high energy trauma. The proximal right tibia displays several fracture planes including a stepped fracture on the medial condyle that, along with other fractures, serve to depress its superior surface inferolaterally. The proximal distal tibial segment displays numerous fractured shaft fragments that were rotated and partially driven into the medullary canal. The tibial plateau and shaft fractures preserve evidence of axial compressive loading. 3D mapping of fracture planes offers a detailed approach to understanding the nature of bone damage.



This lumbar vertebra (Fig. 1) was catalogued as separate fragments: A.L. 288-1aa, # on left lateral edge of centrum; A.L. 288-1ak, # on right posterior surface of arch; and A.L. 288-1al, # on left lateral edge of inferior articular surface. Neither transverse process was recovered. Johanson *et al.* (1982:435) report that "both superior processes were broken away (but have been rejoined) and are in excellent apposition. The same is true for both pedicles."

We agree with Johanson *et al.*'s (1982) description of the location and extent of visible surface cracks but disagree with their conclusion that all breaks are postmortem in nature. We used CT scans (Fig. 2) to map the surface expression of the major cracks through the element (Fig. 3) and these show in 3D the manner in which the pedicles and spinous process were broken. We also show for the first time that the cracks in the centrum communication with one another (Fig. 3) even though the body remained intact. The basivertebral vein is clearly visible in the scans.

One of the most interesting aspects of Lucy's lumbar vertebra is its marked kyphotic wedging (Fig. 1c), plotting well outside the range for modern humans and other fossil hominins (Fig. 4); the L3 of A.L. 288-1 and Sts 14d are similar in size but their wedging angles differ by almost 7°. Although the removal of some bone from the ventral cranial rim of the centrum certainly partially contributes to this high value (Fig. 1a, arrows), the volume shown in red in Fig. 1c is what would have to be removed to attain 0°. Close examination of this surface makes it seem unlikely. CT slices reveal numerous small multi-directional cracks that are more concentrated in the body's ventral than dorsal trabeculae (see especially Fig. 3c-f). These cracks appear to be compressive in nature, and offer evidence for a wedge fracture (Figs. 5 & 6) that damaged the anterior column and was sufficiently severe to produce kyphotic wedging. If this microfracturing had occurred when the bone was dry, it is likely that the body would have been destroyed. Data in Fig. 4 from Sanders (1998), Whitcomb et al. (2007), and Whitcomb (2012).



## Right tibia: proximal segment A.L. 288-1aq; distal segment A.L. 288-1ar

The proximal tibia, A.L. 288-1q (Fig. 7, top), displays numerous cracks described by Johanson *et al.* (1982) as postmortem in nature. Kappelman *et al.* (2016) instead hypothesized that they were caused by perimortem compressive fracturing along the long axis of the shaft resulting from a vertical deceleration event. We used CT scans to map these fractures in 3D. Both tibial condyles are broken, and a prominent fracture runs across the superior surface of the medial condyle anteromedially to end just lateral to the posterior intercondylar area (Figs. 8 & 9, red arrows and line). This fracture depresses its lateral surface inferiorly ~1 mm relative to its medial surface, and appears to have a faint connection with a tall, superoinferiorly oriented fracture on the medioposterior surface of the bone (Figs. 8b & 10, green arrows and line). Other small fractures are also present (Figs. 8b & 10b, yellow and blue lines).

Together these proximal breaks depress the inferolateral aspect of the tibial plateau (Johanson *et al.* 1982), creating an unnatural angle to the shaft with a distinct valgus set that adds about 5° to the average 15° bicondylar angle for *Au. afarensis* (Stern and Susman, 1983). The distinct valgus set (Fig. 11b & c; yellow lines) matches that seen in modern patients who suffer a tibial plateau fracture (Fig. 11c) from a VDE, and is in clear contrast to the similarly-sized but undamaged A.L.129-1b proximal tibia (Fig. 11a, here scaled to the same size as A.L. 288-1q). It appears that the knee's bicondylar angle acted to concentrate more compressive force on the lateral (red arrows in Fig. 11b & c) than medial condyle, creating a fracture pattern that depressed the tibial plateau along its lateral edge.

The distal segment of Lucy's tibia, A.L. 288-1r (Fig. 7 bottom, 12a), preserves numerous cracks, again described as postmortem by Johanson *et al.* (1982) but hypothesized by Kappelman *et al.* (2016) as perimortem. We used CT scans to segment many of the numerous small bone fragments (Fig. 12b). These have sharp, broken edges and, by way of example, the two fragments marked by arrows in Fig. 12b & c were fractured into the medullary canal; the slight CCW rotation of larger of these two fragments (light green arrow) along the long axis of the shaft appears to have broken loose some additional tiny bone chips only a few mms in size that remain at the fracture site (Fig. 12c, yellow arrows). The orientations of these flakes indicate that as the shaft was compressively fractured along its long axis, a torque caused it to buckle and rotate, and it was this combined action that drove the small bone fragments into the medullary canal and produced a spiral fracture.

It appears that the periosteum was in place when the fracture occurred; if the fracture had occurred after the periosteum had decomposed, these tiny fragments would have been lost. Additional support for a perimortem fracture is found in the fact that there is no evidence of healing along any of the sharp fracture edges. Some adhering sandstone matrix remains on the external surface (Fig. 12c white arrow). The fact that the medullary canal is partially mineral-infilled (Fig. 13) and its internal contour round, not stepped as seen along the outer surfaces of the two bone fragments described above, means that these fractures predate the time of infill.

